

## Vertically Aligned Pearl-like Carbon Nanotube Arrays for Fiber Spinning

Huisheng Peng,<sup>\*,†</sup> Menka Jain,<sup>†</sup> Qingwen Li,<sup>†</sup> Dean E. Peterson,<sup>†</sup> Yuntian Zhu,<sup>\*,‡</sup> and Quanxi Jia<sup>\*,†</sup>

*Los Alamos National Laboratory, Los Alamos, New Mexico 87545, and Department of Materials Science and Engineering, North Carolina State University, Raleigh, North Carolina 27695*

Received October 15, 2007; E-mail: hpeng@lanl.gov

Due to their unique structure and physical properties and numerous potential applications, carbon nanotubes have been extensively studied recently and are expected to attract more attention in the future.<sup>1</sup> Morphology control of carbon nanotubes represents one of the most explored directions. Except for the normal linear structure, nanotubes with morphologies of ring,<sup>2</sup> rocket,<sup>2</sup> branch,<sup>3</sup> cone,<sup>4</sup> bulb,<sup>5</sup> star,<sup>6</sup> cup-stacked-type,<sup>7</sup> bamboo,<sup>8</sup> and helix<sup>9</sup> have been widely investigated. Here we first report another new type of nanotubes with a pearl-like morphology. This unique morphology enables nanotubes with much improved fiber spinability. The derived fiber shows excellent mechanical and electrical properties. Furthermore, such nanotubes will be much more effective in reinforcing matrix to produce strong and tough composites.<sup>10</sup>

Chemical vapor deposition (CVD) was used to synthesize pearl-like nanotube arrays (Figure 1). Experimental details are described in the Supporting Information. Arrays with thickness up to hundreds of micrometers can be prepared by this approach. The as-synthesized carbon nanotubes are highly aligned with each other in the array, as demonstrated by scanning electron microscopy (SEM) and X-ray diffraction (XRD). Figure 2a shows that the top surface of as-synthesized arrays is uniform and flat. The vertically aligned carbon nanotubes can be clearly observed from a side view (inserted image in Figure 2a and Figure S1). The preferentially aligned arrays are further confirmed by XRD.<sup>11</sup> When the incident X-ray strikes arrays from the top, only a weak peak of (100) at 42.4° is observed, which corresponds to a crystal spacing of 2.12 nm (Figure S2a); however, when the incident X-ray comes at the side direction of the same sample, a much stronger peak of (002) emerges and corresponds to the interplanar spacing of 0.34 nm (Figure S2b). The XRD results also indicate that the synthesized nanotubes are multiwalled.

Nanotube arrays are further characterized by Raman spectroscopy (Figure 2b). For normal linear nanotubes, the strong D-band corresponds to the disorder features due to the finite particle size effect or lattice distortion of the graphite crystals.<sup>12</sup> For these pearl-like carbon nanotubes, a major contribution also comes from the distortion in the connection segment between "bulb" and "trunk" parts.

The pearl-like morphology of synthesized carbon nanotubes is studied by transmission electron microscopy (TEM). As shown in Figure 3a and 3b, the diameter of the trunk part is 23 nm, and the maximum diameter for bulb parts is 39 nm. Diameters of the hollow part in the bulb and trunk are 9 and 15–22 nm, respectively. High-resolution TEM image in Figure 3c further confirms the multiwalled structure of the pearl-like nanotubes. More details can be found in the Supporting Information.

Deriving a detailed mechanism for the formation of such a pearl-like structure is still a challenge. We have observed that the pearl-

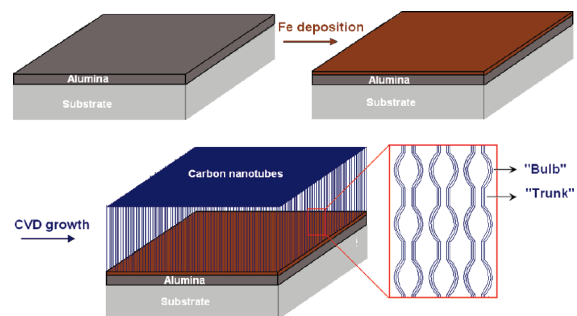


**Figure 1.** Synthesis of the pearl-like carbon nanotube arrays through a chemical vapor deposition (CVD) process.

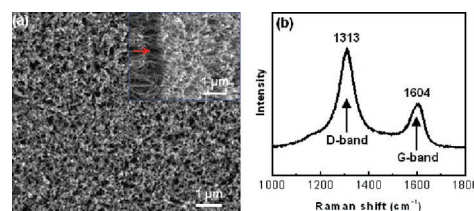


**Figure 2.** Highly aligned carbon nanotube arrays. (a) Top view by SEM (inserted, side view shown by the red arrow). (b) Raman spectrum.

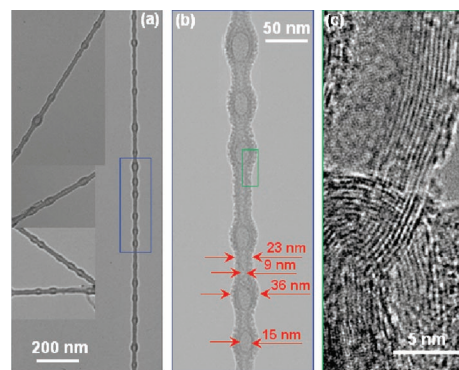


**Figure 3.** (a and b) TEM images of pearl-like nanotubes. (c) High-resolution TEM image of pearl-like nanotubes.

like structure can be formed only at the temperature range of 800–850 °C. The catalyst particles are in a solid–liquid two-phase state in this temperature range.<sup>13</sup> It has also been reported that the size and geometry of the catalytic particle largely control the size and morphology of carbon nanotubes.<sup>13,14</sup> On the basis of this evidence, we propose a dynamic solid–liquid oscillation mechanism for the formation of the pearl-like nanotubes. According to the C–Fe phase diagram,<sup>13</sup> the catalyst particle will transform to the liquid state when the carbon content is high and to the solid state when it is low. It has also been known that carbon atoms diffuse to the catalyst–nanotube interface to sustain the nanotube growth. Assume that the catalyst particle is initially in the solid state. The solid catalyst particle tends to take a spherical shape to lower its surface

<sup>†</sup> Los Alamos National Laboratory.

<sup>‡</sup> North Carolina State University.

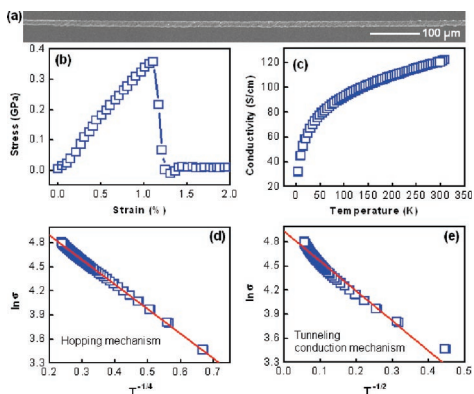


**Figure 4.** (a) SEM image of a fiber spun from pearl-like nanotube arrays. (b) Mechanical test. (c) Temperature dependence of the fiber conductivity. (d) Scaling of the conductivity data with the variable range hopping mechanism on a plot of  $\ln \sigma$  versus  $T^{-1/4}$ . (e) Scaling of the conductivity data with the tunneling conduction mechanism on a plot of  $\ln \sigma$  versus  $T^{-1/2}$ .

energy, which produces a big tube diameter. The diffusion of carbon atoms is slow in the solid catalyst. If the supply of carbon atoms to the catalytic particle is faster than their diffusion, the carbon content in the particle will increase, transforming part or all of the particle into the liquid state. A liquid catalyst particle tends to take an oblong shape, producing a smaller diameter. The diffusion is much faster in a liquid catalyst particle, which makes the nanotube grow much faster and consequently lower the carbon content in the catalyst particle. This transforms it back to the solid state. The repetition of the above process produces a pearl-like structure. Such a mechanism can only happen in a narrow temperature range in which the solid–liquid transformation occurs. Note that, due to the changing transformation speed of the catalytic particle during the nanotube growth,<sup>15</sup> the distance between two neighboring bulbs varies (Figure 3a and 3b). Further study is underway.

To fully utilize the unique physical properties of carbon nanotubes, it is desirable to spin them into continuous fibers at macroscopic scale.<sup>16</sup> However, the continuous spinning is challenging due to the slide among linear carbon nanotubes that originated from their smooth cylindrical outer surface. As expected, the unique pearl-like morphology in the present system provides much improved spinning ability. The pearl-like nanotube arrays can be easily spun into long fibers. Figure 4a shows the typical photograph of a derived fiber. These fibers exhibit a maximum tensile strength of 0.35 GPa (Figure 4b), higher than 0.15–0.18 GPa of fibers spun from normal linear nanotubes synthesized at 750 °C. The tensile strength can be further improved to 1.24 GPa after wetting with polydiacetylenes. These fibers also show excellent electrical property. Their electrical conductivity is 250 S/cm at room temperature. Figure 4c further reveals the temperature dependence of the conductivity of a fiber from 190 to 300 K. The conductivity increases from 32 S/cm at 5 K to 122 S/cm at 310 K, indicating a semiconducting behavior of the fibers derived from the pearl-like nanotubes.

For the temperature dependence of conductivity, two main mechanisms have been suggested, that is, a variable range hopping mechanism<sup>17a,b</sup> and a tunneling conduction mechanism.<sup>17a,c</sup> These two mechanisms are respectively described by the following two equations:  $\sigma = \sigma_0 \exp(-A/T^{1/4})$  and  $\sigma = \sigma_0 \exp(-B/T^{1/2})$ , where  $\sigma$  is the electrical conductivity,  $\sigma_0$ ,  $A$ , and  $B$  are constants, and  $T$  is the temperature. As shown in Figure 4d and 4e,  $\ln \sigma$  versus  $T^{-1/4}$  based on the first equation shows a much higher degree of linearity in a wider range than that of  $\ln \sigma$  versus  $T^{-1/2}$  based on the second equation. This indicates that the conduction in this system is mainly

controlled by the three-dimensional hopping mechanism. This behavior is most likely due to the unique morphology of these pearl-like nanotubes, in which electrons cannot be confined in the 1D channel as normal linear nanotubes.

Carbon nanotubes have also been proposed as nanoreactors due to the well-defined structure in terms of inner hollow cavities and a high aspect ratio.<sup>18</sup> Some successful applications have been reported.<sup>18,19</sup> Due to the different sizes of the bulb and trunk, these pearl-like nanotubes may find new applications by introducing other components into either the bulb or the trunk parts. More research is underway to incorporate metals and monomers into the bulbs of the pearl-like nanotubes.

In summary, we have demonstrated the first synthesis of well-aligned, pearl-like carbon nanotube arrays through a CVD process. Due to the unique morphology, these carbon nanotubes can be easily spun into macroscopic fibers with excellent mechanical and electrical properties. In addition, the interesting hollow structure inside the nanotube may open new applications for carbon nanotubes as nanoreactors.

**Acknowledgment.** This work was supported as a Los Alamos National Laboratory Directed Research and Development Project under the United States Department of Energy.

**Supporting Information Available:** Structure, property, and mechanism of pearl-like nanotubes. This material is available free of charge via the Internet at <http://pubs.acs.org>.

## References

- (1) (a) Ren, Z. F.; Huang, Z. P.; Xu, J. W.; Wang, J. H.; Bush, P.; Siegal, M. P.; Provencio, P. N. *Science* **1998**, *282*, 1105–1107. (b) Chen, W.; Dai, L.; Roy, A.; Tolle, T. B. *J. Am. Chem. Soc.* **2006**, *128*, 1412–1413.
- (2) Cohen, A. E.; Mahadevan, L. *Proc. Natl. Acad. Sci. U.S.A.* **2003**, *100*, 12141–12146.
- (3) Meng, G.; Jung, Y. J.; Cao, A.; Vajtai, R.; Ajayan, P. M. *Proc. Natl. Acad. Sci. U.S.A.* **2005**, *102*, 7074–7078.
- (4) Zhang, G.; Jiang, X.; Wang, E. *Science* **2003**, *300*, 472–474.
- (5) de Heer, W. A.; Poncharal, P.; Berger, C.; Gezo, J.; Song, Z.; Bettini, J.; Ugarte, D. *Science* **2005**, *307*, 907–910.
- (6) Sano, M.; Kamino, A.; Shinkai, S. *Angew. Chem., Int. Ed.* **2001**, *40*, 4661–4663.
- (7) Endo, M.; et al. *Appl. Phys. Lett.* **2002**, *80*, 1267–1269.
- (8) Xiong, Y.; Li, Z.; Guo, Q.; Xie, Y. *Inorg. Chem. Mater.* **2005**, *44*, 6506–6508.
- (9) Hou, H.; Jun, Z.; Weller, F.; Greiner, A. *Chem. Mater.* **2003**, *15*, 3170–3175.
- (10) (a) Xu, T. T.; Fisher, F. T.; Brinson, L. C.; Ruoff, R. S. *Nano Lett.* **2003**, *3*, 1135–1139. (b) Lao, J. Y.; Li, Y. Z.; Wen, J. G.; Ren, Z. F. *Appl. Phys. Lett.* **2002**, *80*, 500–502.
- (11) Cao, A.; Xu, C.; Liang, J.; Wu, D.; Wei, B. *Chem. Phys. Lett.* **2001**, *344*, 13–17.
- (12) Luo, T.; Liu, J.; Chen, L.; Zeng, S.; Qian, Y. *Carbon* **2005**, *43*, 755–759.
- (13) Jiang, K.; Feng, C.; Liu, K.; Fan, S. *J. Nanosci. Nanotechnol.* **2007**, *7*, 1494–1504.
- (14) (a) Xia, W.; Su, D.; Schlogl, R.; Birkner, A.; Muhler, M. *Adv. Mater.* **2005**, *17*, 1677–1679. (b) Hu, J.; Bando, Y.; Zhan, J.; Zhi, C.; Xu, F.; Golberg, D. *Adv. Mater.* **2006**, *18*, 197–200. (c) Bhimarasetti, G.; Sunkara, M. K.; Graham, U. M.; Davis, B. H.; Suh, C.; Rajan, K. *Adv. Mater.* **2003**, *15*, 1629–1632.
- (15) Lin, M.; Tan, J. P. Y.; Boothroyd, C.; Loh, K. P.; Tok, E. S.; Foo, Y.-L. *Nano Lett.* **2007**, *7*, 2234–2238.
- (16) (a) Zhang, M.; Fang, S.; Zakhidov, A. A.; Lee, S. B.; Aliev, A. E.; Williams, C. D.; Atkinson, K. R.; Baughman, R. H. *Science* **2005**, *309*, 1215–1219. (b) Ericson, L. M.; et al. *Science* **2004**, *305*, 1447–1450. (c) Vigolo, B.; Penicaud, A.; Coulon, C.; Sauder, C.; Paillet, R.; Journet, C.; Bernier, P.; Poulin, P. *Science* **2000**, *290*, 1331–1334. (d) Jiang, K.; Li, Q.; Fan, S. *Nature* **2002**, *419*, 801.
- (17) (a) Li, Q.; et al. *Adv. Mater.* **2007**, *19*, 3358–3363. (b) Banerjee, S.; Chakravorty, D. *J. Appl. Phys.* **1998**, *84*, 1149–1151. (c) Ma, Y. G.; Liu, H. J.; Ong, C. K. *Europhys. Lett.* **2006**, *76*, 1144–1150.
- (18) Chen, W.; Pan, X.; Willinger, M.-G.; Su, D. X.; Bao, X. *J. Am. Chem. Soc.* **2006**, *128*, 3136–3137.
- (19) (a) Sun, X. H.; Li, C. P.; Wong, W. K.; Wong, N. B.; Lee, C. S.; Lee, S. T.; Teo, B. K. *J. Am. Chem. Soc.* **2002**, *124*, 14464–14471. (b) Nhut, J. M.; Pesant, L.; Tessonnier, J. P.; Wine, G.; Guille, J.; Pham-Huu, C.; Ledoux, M. *J. Appl. Catal. A* **2003**, *254*, 345–363.

JA077767C